

# Collisions between solitary waves of three-dimensional Bose-Einstein condensates

N.G. Parker<sup>1,2</sup>, A. M. Martin<sup>1</sup>, S. L. Cornish<sup>2</sup> and C. S. Adams<sup>2</sup>

<sup>1</sup> *School of Physics, University of Melbourne, Parkville, Victoria 3010, Australia*

<sup>2</sup> *Department of Physics, University of Durham, South Road, Durham, DH1 3LE, United Kingdom*

We study bright solitary waves of three dimensional trapped Bose-Einstein condensates and their collisions. For a single solitary wave, in addition to an upper critical number, we also find a *lower* cut-off, below which no stable state can be found. Collisions between solitary waves can be elastic, inelastic with either reduced or increased outgoing speed, or completely unstable due to a collapse instability. A  $\pi$ -phase difference between the waves promotes elastic collisions, and gives excellent agreement with recent experimental results over long timescales.

PACS numbers: 03.75.Lm, 03.75.Hh, 05.45.Yv

Bright solitary waves (BSWs) of atomic Bose-Einstein condensates (BECs) have been observed in the form of a single BSW [1] and groups of interacting BSWs [2, 3] for attractive atomic interactions, and as gap BSWs in periodically-confined BECs with repulsive interactions [4]. In the former case, the attractive interactions which support the BSW against dispersion also induce a collapse instability when the number of atoms exceeds a critical value  $N_C$  [5, 6], making attractive BECs problematic to form. Consequently, ‘soliton’ experiments first form a stable BEC with repulsive atomic interactions and switch to attractive interactions by means of the molecular Feshbach resonance [7]. For  $N < N_C$ , a single BSW forms [1], while for  $N > N_C$  a ‘bosonova’-type collapse instability [6, 8, 9] is induced with excess atoms being ejected from the condensate. The ‘remnant’ condensate is observed to contain BSWs [2, 3] which oscillate in the trap and interact with each other. It has been inferred [2] that the BSWs repel each other due to  $\pi$ -phase differences between them, thought to be formed by modulational instability of the condensate [2, 10, 11]. With matter-wave ‘solitons’ being potential candidates for applications such as interferometry and quantum information processing, a thorough understanding of their properties and in particular their *interactions* is of key importance.

Theoretically, bright solitons are stable solutions of the 1D nonlinear Schrödinger equation with a sech-shaped wave profile [12]. In isolation their form is preserved by a balance between dispersion and attractive nonlinearity, and they can have any population. Another key property is that they emerge from collisions with unchanged form. However, even in 1D, the exact collisional form depends on the relative phase between the incoming solitons  $\Delta\phi$  [13]: for  $\Delta\phi = 0$  the waves can overlap completely (attractive solitonic interaction), while for  $\Delta\phi = \pi$  no overlap can occur and the solitons appear to ‘bounce’ (repulsive solitonic interaction). BSWs, the 3D analog of the bright soliton, may have considerably different properties: the existence of multiple dimensions leads to the collapse instability [5, 9] and thermal dissipation [14]. Indeed, two colliding BSWs can form a high-density state unstable to collapse, with relative phase difference playing a key role [11, 15]. Whereas the experiments of [1, 2]

use highly-elongated ‘quasi-1D’ geometries, Cornish *et al.* [3] employ a very weakly-elongated geometry, and, somewhat surprisingly, observe well-behaved BSW oscillations for very long times with negligible damping. This raises questions over how ‘solitonic’ such 3D states are.

In 3D an untrapped attractive BEC is always unstable to collapse [16]. Addition of confinement can stabilise it up to a critical density and number of atoms  $N_C$  [6, 17, 18, 19]. By definition a BSW should be capable of axial self-trapping. In the absence of external axial trapping, radial confinement is necessary to make  $N_C$  finite, and also to enable approximation to a 1D soliton.

In this work we simulate BSWs of 3D BECs and their collisions. We observe rich and complex dynamics, which extend well beyond the 1D soliton. Below a *lower* critical atom number we show that stable BSW solutions do not exist. Collisions can be elastic, inelastic with increased or decreased speed, or completely destructive. We highlight the effect of relative phase, number of atoms and speed on the collisional stability. Furthermore we show that recent observations of Cornish *et al.* [3] are consistent with two oscillating BSWs with  $\pi$ -phase difference, with the simulations giving excellent agreement with the experimental oscillation data, over long timescales (for over 20 oscillations/3 seconds), despite neglecting higher-order effects such as thermal dissipation [14].

We employ the Gross-Pitaevskii equation (GPE) to describe the condensate mean-field ‘wavefunction’  $\psi(\mathbf{r}, t)$ ,

$$i\hbar\frac{\partial\psi}{\partial t} = \left[ -\frac{\hbar^2}{2m}\nabla^2 + \frac{1}{2}m(\omega_r^2 r^2 + \omega_z^2 z^2) + g|\psi|^2 \right] \psi. \quad (1)$$

Here  $m$  is the atomic mass and  $g = 4\pi\hbar^2 a_S/m$  is the interaction coefficient, where  $a_S$  is the  $s$ -wave scattering length ( $a_S < 0$  in this study, corresponding to attractive atomic interactions). The harmonic confining potential is cylindrically-symmetric with  $z$  and  $r$  representing the axial and radial coordinates. We base our analysis on the <sup>85</sup>Rb experiment [3] with scattering length  $a_S = -0.6$  nm and radial trap frequency  $\omega_r = 2\pi \times 17.5$  Hz.

We begin by considering isolated BSW solutions. To generate such states we propagate the GPE in imaginary time subject to the desired atom number  $N_S$  and exter-

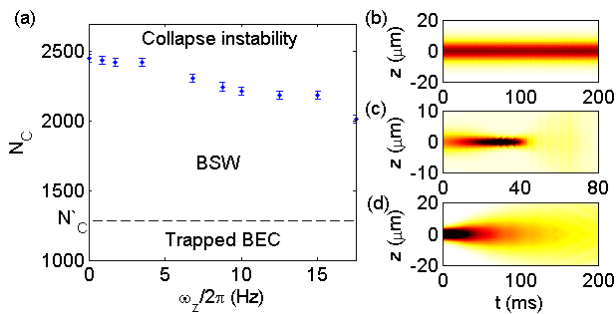


FIG. 1: (a) Upper critical number  $N_C$  as a function of  $\omega_z$  ( $\omega_r = 2\pi \times 17.5$  Hz). Indicated are the lower critical number  $N'_C$  for  $\omega_z = 0$  (dashed line) and the condensate regimes. (b) Radially-integrated axial density versus time for a BSW ( $N_S = 1500$ ) with  $\omega_z = 0$ . (c)-(d) Same as (b) but with initial density rescaled to (c)  $N_S = 2700$  and (d)  $N_S = 1000$ . Dark/light regions represent high/low density.

nal potential [20]. Following previous studies [17, 18] we isolate the critical number for collapse  $N_C$  when the GPE no longer converges to a solution. Figure 1(a) shows the critical number  $N_C$  as a function of axial trap frequency  $\omega_z$ . For an axially-homogeneous system we find a range of values of  $N_S$  where solutions exist which are axially self-trapping (Fig. 1(b)), i.e. BSW solutions. For  $N_S > N_C = (2450 \pm 30)$  the wavepacket is unstable to interaction-induced collapse, followed by explosive dynamics (Fig. 1(c)). In addition to the upper critical number we also find a lower critical regime when  $N_S < N'_C = (1280 \pm 20)$ . For  $N_S < N'_C$  the wavepacket is no longer self-trapped axially but spreads over time (Fig. 1(d)), since the attractive interactions are no longer sufficient to prevent dispersion of the wave. Both the low- $N_S$  and high- $N_S$  instabilities do not occur for the 1D soliton, which is robust to any population.

Under axial confinement  $N_C$  decreases weakly with  $\omega_z$ . The axial trapping increases the peak density [21], making the BSW more prone to the collapse instability. For  $\omega_z = 2\pi \times 6.8$  Hz [3] we find  $N_C = (2305 \pm 30)$ , in excellent agreement with experimental observations of  $N_C \approx (2284 \pm 300)$  [6]. Alternative approaches have previously over or under estimated  $N_C$  [18, 19].

Axial confinement provides a sufficient restoring force to axially trap the condensates and achieve stable solutions for  $N < N'_C$ . However, such a state can no longer be classed as a BSW because it is not capable of axial self-trapping; it is then simply the ground state trapped attractive BEC. The regimes of the attractive system, i.e. instability to collapse, stable BSW, and trapped BEC, are indicated in Fig. 1(a). The states observed in [3] appear to have a population in the range  $N'_C < N < N_C$ , consistent with being BSWs.

We now consider collisions between two BSWs, each with  $N_S = 1500$ , in an axially-homogeneous system. In 1D this collision is stable and elastic. Initially the BSWs are well-separated and given an axial momentum kick,  $\psi = |\psi| \exp(imv_{in}z/\hbar)$ , such that they propagate towards

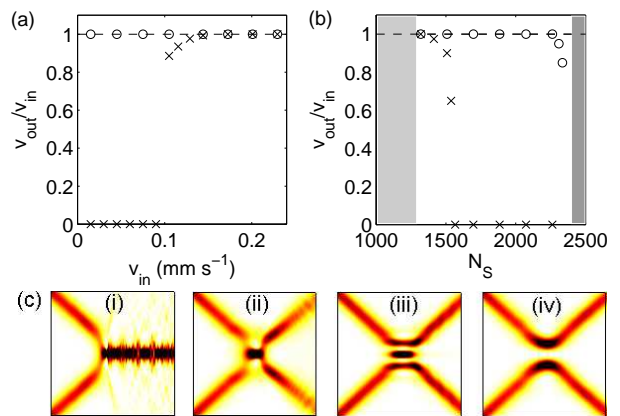


FIG. 2: (a)-(b)  $v_{out}/v_{in}$  for a BSW collision with  $\Delta\phi = 0$  (crosses) and  $\Delta\phi = \pi$  (circles) in a  $\omega_z = 0$  ( $\omega_r = 2\pi \times 17.5$  Hz) system as a function of (a) incoming speed  $v_{in}$  ( $N_S = 1500$ ), and (b) atom number  $N_S$  ( $v_{in} = 0.12 \text{ mm s}^{-1}$ ). The dashed line represents  $v_{out} = v_{in}$ . In the shaded regions BSW solutions are not accessible (light region:  $N_S < N'_C$ ; dark region:  $N_S > N_C$ ). (c) Axial density (integrated over  $r$ ) as a function of  $v_{in}t$  for (i)  $\Delta\phi = 0$  and  $v_{in} = 0.03 \text{ mm s}^{-1}$ , (ii)  $\Delta\phi = 0$  and  $v_{in} = 0.09 \text{ mm s}^{-1}$ , (iii)  $\Delta\phi = 0$  and  $v_{in} = 0.24 \text{ mm s}^{-1}$ , and (iv)  $\Delta\phi = \pi$  and  $v_{in} = 0.09 \text{ mm s}^{-1}$ . Each box represents the region  $[0, 80 \mu\text{m}/v_{in}] \times [-40, 40] \mu\text{m}$ .

each other with speed  $v_{in}$ . In isolation the BSWs propagate with constant speed and shape (see early times in Fig. 2(c)). We also control the phase difference  $\Delta\phi$  between the BSWs by initially multiplying one BSW by  $\exp(i\Delta\phi)$ . We primarily consider the extreme cases of  $\Delta\phi = 0$  and  $\pi$ . We consider speeds of the order of those observed experimentally [3]: assuming an amplitude  $z_0 \sim 10 \mu\text{m}$  in the trap, harmonic motion suggests a maximum speed  $v = \omega_z z_0 \sim 0.4 \text{ mm s}^{-1}$ .

We parameterise the stability of a BSW collision in terms of the outgoing speed  $v_{out}$ . Figure 2(a) plots the ratio  $v_{out}/v_{in}$  as a function of incoming speed  $v_{in}$  for the cases of  $\Delta\phi = 0$  (crosses) and  $\Delta\phi = \pi$  (circles). For  $\Delta\phi = 0$  and low  $v_{in}$  ( $v_{in} \lesssim 0.09 \text{ mm s}^{-1}$ ), the BSWs do not emerge from the collision (Fig. 2(c)(i)) [22]. The overlap of the BSWs forms an intermediate state with sufficiently high density that a destructive bosonova-like collapse instability is induced [9, 11, 15]. For  $\Delta\phi = 0$  and intermediate  $v_{in}$  ( $0.1 \lesssim v_{in} \lesssim 0.14 \text{ mm s}^{-1}$ ), BSWs emerge from the collision but with  $v_{out} < v_{in}$ . The density again reaches a critical level, but only a *partial* collapse instability is induced (Fig. 2(c)(ii)). This leads to an irreversible transfer of energy from centre-of-mass kinetic energy to excite 3D collective modes of the BSWs. As the  $v_{in}$  is increased further the collision becomes more elastic ( $v_{out} \rightarrow v_{in}$ ) and the shape excitations become negligible. These elastic dynamics, shown in Fig. 2(c)(iii), illustrate how the BSWs pass through each other and form 3 fringes in a stable  $\Delta\phi = 0$  collision. This limit is analogous to the corresponding 1D soliton collision.

In contrast,  $\Delta\phi = \pi$  collisions are elastic throughout this range of  $v_{in}$ . Overlap of the BSWs at the centre of

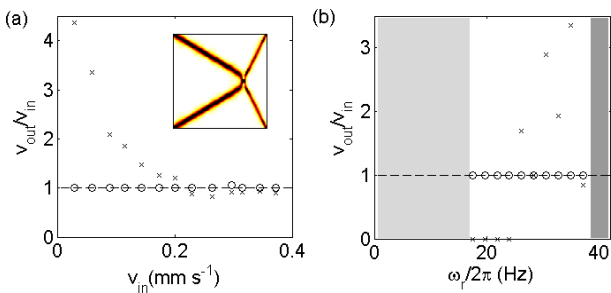


FIG. 3: (a)-(b) Ratio  $v_{\text{out}}/v_{\text{in}}$  of a BSW collision with  $\Delta\phi = 0$  (crosses) and  $\Delta\phi = \pi$  (circles) in a  $\omega_z = 0$  system as a function of (a)  $v_{\text{in}}$  (for  $\omega_r = 2\pi \times 35$  Hz and  $N_S = 1500$ ) and (b)  $\omega_r$  (for  $v_{\text{in}} = 0.06$  mms $^{-1}$  and  $N_S = 1500$ ). The dashed lines plot  $v_{\text{out}} = v_{\text{in}}$ . Inset in (a): axial density (integrated over  $r$ ) as a function of  $v_{\text{in}}t$  for  $\Delta\phi = 0$ ,  $v_{\text{in}} = 0.06$  mms $^{-1}$  and  $\omega_r = 2\pi \times 35$  Hz. The box represents the region  $[-40, 40]$   $\mu\text{m} \times [0, 50 \mu\text{m}/v_{\text{in}}]$ . In the shaded regions of (b) BSW solutions are not accessible (light region:  $N_S < N'_C$ ; dark region:  $N_S > N'_C$ ).

mass is prevented and the BSWs ‘bounce’ (Fig. 2(c)(iv)). This restricts the increase of the peak density during the collision [23], and stabilises against instability [11].

From the solutions generated in Fig. 1(a) for  $\omega_z = 0$  we estimate the critical density for collapse to be  $n_C \sim 5 \times 10^{19}$  m $^{-3}$ . All of the  $\Delta\phi = 0$  collisions in Fig. 2(a) exceed this density, while the  $\Delta\phi = \pi$  collisions do not. The stabilisation of collisions with speed suggests that the *timescale* plays a key role. Indeed, in the elastic (inelastic) regime  $v_{\text{in}} \gtrsim 0.15$  mms $^{-1}$  ( $v_{\text{in}} \lesssim 0.15$  mms $^{-1}$ ) the time over which  $n_C$  is exceeded becomes consistently less (greater) than around 5 ms, which is the characteristic collapse time observed experimentally [9].

The stability is also sensitive to atom number  $N_S$ . Figure 2(b) shows  $v_{\text{out}}/v_{\text{in}}$  as a function of  $N_S$  ( $v_{\text{in}} = 0.12$  mms $^{-1}$ ). Addition of atoms makes the BSW more prone to the collapse instability, destabilising the collisions with increasing  $N_S$ . For  $\Delta\phi = 0$  the collisions break down for low  $N_S$  ( $N_S \sim 1400$ ) while the  $\Delta\phi = \pi$  collision remains elastic up until just below  $N_C$ .

For  $0 < \Delta\phi < \pi$  the degree of overlap during the collision varies between full overlap ( $\Delta\phi = 0$ ) and no overlap ( $\Delta\phi = \pi$ ). Population transfer occurs between the BSWs, with the outgoing speeds becoming asymmetric to conserve momentum, complicating the dynamics. Although we concentrate here on  $\Delta\phi = 0$  and  $\pi$  we have tested their robustness by considering 10% deviations of each ( $\Delta\phi = 0.1\pi$  and  $0.9\pi$ ), and observe that the regimes of stability are robust to such variations [24].

We now double the radial trap frequency to  $\omega_r = 2\pi \times 35$  Hz. The collisional stability as a function of incoming speed is shown in Fig. 3(a). For low  $v_{\text{in}}$  we again observe inelastic collisions, but this time  $v_{\text{out}} > v_{\text{in}}$  ( $v_{\text{out}}/v_{\text{in}} \lesssim 4.5$ ). As the incoming speed is increased further the collision becomes more elastic ( $v_{\text{out}} \rightarrow v_{\text{in}}$ ), as seen previously in Fig. 2(a). A low speed inelastic collision with  $v_{\text{out}}/v_{\text{in}} \approx 3.3$  is shown in Fig. 3(a)(inset).

During the collision the high density triggers a partial collapse instability. A small fraction of atoms (around 10% in this case) are ejected from the BSWs, releasing a significant amount of interaction energy which is converted into kinetic energy. For lower  $\omega_r$  this would tend to generate a radial burst of highly-energetic atoms (bosenova) [9]. However for sufficiently high  $\omega_r$  we propose that this radial burst is suppressed, with a significant fraction of this kinetic energy focussed axially into the BSWs, thereby increasing their speed. Again, for  $\Delta\phi = \pi$  the collisions remain elastic throughout this range of speeds.

In Fig. 3(b) we vary the radial trap frequency  $\omega_r$  while keeping  $N_S$  fixed. We observe BSW destruction for  $\Delta\phi = 0$  and low  $\omega_r$  (3D bosenova instability), while for larger  $\omega_r$  we typically see the ratio  $v_{\text{out}}/v_{\text{in}}$  grow. There is occasionally no speed increase, highlighting the sensitivity of this highly nonlinear effect. The  $\Delta\phi = \pi$  collisions remain elastic. For  $\omega_r \sim 2\pi \times 38$  Hz,  $N_C$  decreases to  $N_S$  and we cannot generate BSW solutions beyond this. If  $N_C$  is not exceeded all collisions should become elastic in the quasi-1D limit of large  $\omega_r$ .

In addition to radial trapping ( $\omega_r = 2\pi \times 17.5$  Hz) we now add axial confinement  $\omega_z = 2\pi \times 6.84$  Hz to compare with experiments [3]. Note we have slightly modified  $\omega_z$  from the quoted experimental value of  $\omega_z = 2\pi \times 6.8$  Hz in order to match the experimental data, as we will see. It was observed that the number of atoms left in the condensate remnant was greater than  $N_C$ , and divided between two states, each with population  $N_S < N_C$ , which oscillate axially. We continue to employ  $N_S = 1500$ , which satisfies these conditions. Note that the collapse-induced conversion of interaction into kinetic energy discussed above may explain the formation of oscillating BSWs in the experiment rather than stationary ones. The BSWs are positioned at  $z_0 = \pm 14 \mu\text{m}$ . We no longer apply a momentum kick since the trap accelerates the BSWs. The dynamics at *early times* for the cases of  $\Delta\phi = 0$  and  $\Delta\phi = \pi$  are shown in Fig. 4(a) and (b) respectively. Initially the BSWs accelerate identically towards the trap centre. As they interact we see the different collisional dynamics, with the BSWs overlapping for  $\Delta\phi = 0$  and ‘bouncing’ for  $\Delta\phi = \pi$ . However, at these early times the overall dynamics for both cases are similar: the BSWs emerge from the collisions with large collective excitations being generated. In Fig. 4(c) we plot the early evolution of the axial full width half maximum FWHM (related to a gaussian fit) of the  $\Delta\phi = 0$  (dashed line) and  $\Delta\phi = \pi$  (solid line) systems and compare with the experimental data [3] (circles). At early times there is little difference between the  $\Delta\phi = 0$  and  $\pi$  dynamics. The dominant feature in both the experimental and numerical data is an oscillation at  $2\omega_z$ , corresponding to the centre-of-mass oscillations of the BSWs. We have chosen the initial BSW separation to approximately match the maximum experimental widths. The experimental widths decrease to around  $18 \mu\text{m}$  which represents the resolution limit of the measurements. The numerical minima occur at  $\text{FWHM} \sim 2-5 \mu\text{m}$  (this is typically larger for  $\Delta\phi = \pi$

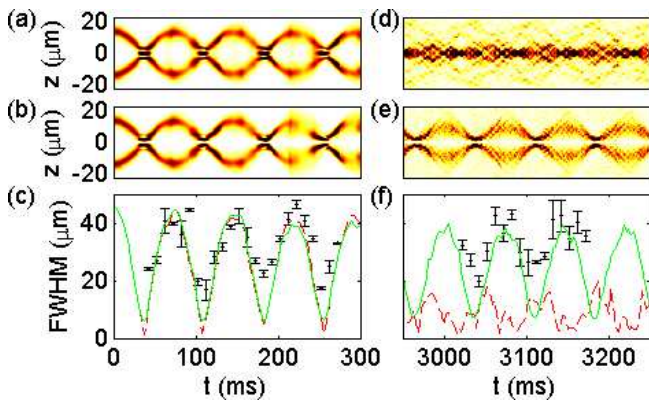


FIG. 4: (a)-(b) Evolution of the radially-integrated axial density at early times for two BSWs ( $N_S = 1500$  and initial amplitude  $z_0 = \pm 14 \mu\text{m}$ ) with (a)  $\Delta\phi = 0$  and (b)  $\Delta\phi = \pi$  ( $\omega_z = 2\pi \times 6.84$  Hz and  $\omega_r = 2\pi \times 17.5$  Hz). (c) Full-width-half-maximum FWHM of a gaussian fit to the axial density for  $\Delta\phi = 0$  (dashed line),  $\Delta\phi = \pi$  (solid line), and experimental data (points) [3]. Note we have time-shifted the experimental data to match the phase of the oscillations at early times. (d)-(f) Same as (a)-(c) but for late times.

due to the repulsive nature of the interaction). Whereas our simulations begin at maximum widths, the experimental data begins at a minimum [3], indicating that the BSWs are created in close proximity. Note that in order to match the phase of the oscillations in Fig. 4(c) we have shifted the experimental data in time.

We do not detect the secondary  $2\omega_r$  frequency component observed experimentally. However, atoms ejected during the initial experimental collapse lead to a significant oscillation at  $2\omega_r$  [3]. Furthermore we have verified that any offset of the BSWs from the  $z$ -axis will induce a  $2\omega_r$  oscillation. The second largest frequency component in the simulations occurs at  $\omega \approx 2\pi \times 27$  Hz with an amplitude of only around 5% of the  $2\omega_z$  component, and arises from the collective modes excited in the BSWs.

Importantly, the experiment oscillations were observed for over 3 s with no discernable damping [3]. The dynamics at *late* times are shown in Fig. 4(d)-(f). The repeated collisions gradually destabilise the collisions through the

growth of collective excitations. Partial collapse instabilities eject highly energetic atoms from the BSWs, which leads to the formation of a diffuse spread of low density ‘hot’ atoms. The  $\Delta\phi = 0$  case is most prone to instability, and by late times the BSWs have collapsed to a central highly-unstable wavepacket (Fig. 4(c)). The FWHM for this case lies well below the experimental values (Fig. 4(f), dashed line). For  $\Delta\phi = \pi$ , two oscillating wavepackets persist at late times, albeit in highly-excited states (Fig. 4(e)). The FWHM for  $\Delta\phi = \pi$  (Fig. 4(f), solid line) remains close to the experimental values even at these late times. Note that in order to match the phase of the experimental data at late times we find it necessary to modify the quoted experimental axial trap frequency by around 0.5% to  $\omega_z = 2\pi \times 6.84$  Hz. This agrees well with the *fitted* frequency in the experiment [3], and implies that the BSW oscillations are an accurate measurement of trap oscillation frequency.

In conclusion we find that bright solitary waves exhibit rich and complex behaviour, not present for 1D solitons. We observe not just the upper critical population familiar with trapped attractive BECs but also a *lower* critical population, below which the wavepacket is no longer capable of axially self-trapping. High-density collisions between BSWs induce instabilities. For large instability the BSWs are destroyed by a catastrophic collapse. For intermediate instability the collisions are inelastic, with *higher* or *lower* outgoing speed. We highlight the sensitive dependence of the instability on the phase difference between the BSWs, collisional speed, atomic population, and trap geometry, all of which are controllable experimentally. In particular elastic collisions are promoted for a  $\pi$ -phase difference between the BSWs and high collisional speeds. Furthermore, we find that the experimental observations of long-lived ‘soliton’ oscillations by Cornish *et al.* [3] are successfully modelled in terms of two oscillating BSWs with a  $\pi$ -phase difference.

We acknowledge the UK EPSRC (NGP/CSA), Royal Society (SLC), University of Melbourne (NGP/AMM) and ARC (NGP/AMM) for support. We thank S. A. Gardiner and J. Brand for discussions.

- 
- [1] L. Khaykovich *et al.*, Science **296**, 1290 (2002).  
[2] K. E. Strecker *et al.*, Nature **417**, 150 (2002).  
[3] S. L. Cornish, S. T. Thompson, and C. E. Wieman, cond-mat/0601664.  
[4] B. Eiermann *et al.*, Phys. Rev. Lett. **92**, 230401 (2004).  
[5] C. C. Bradley, C. A. Sackett, and R. G. Hulet, Phys. Rev. Lett. **78**, 985 (1997).  
[6] J. L. Roberts *et al.*, Phys. Rev. Lett. **86**, 4211 (2001).  
[7] S. L. Cornish *et al.*, Phys. Rev. Lett. **85**, 001795 (2000).  
[8] J. M. Gerton, D. Strekalov, I. Prodan, and R. G. Hulet, Nature (London) **408**, 692 (2000).  
[9] E. A. Donley *et al.*, Nature **412**, 295 (2001).  
[10] U. Al Khawaja *et al.*, Phys. Rev. Lett. **89**, 200404 (2002); L. Salasnich, A. Parola, and L. Reatto, Phys. Rev. Lett. **91**, 080405 (2003).  
[11] L. D. Carr and J. Brand, Phys. Rev. Lett. **92**, 040401 (2004).  
[12] V. E. Zakharov and A. B. Shabat, Sov. Phys. JETP **34**, 62 (1971).  
[13] J. P. Gordon, Opt. Lett. **8**, 596 (1983).  
[14] S. Sinha, A. Y. Cherny, D. Kovrizhin, and J. Brand, Phys. Rev. Lett. **96**, 030406 (2006).  
[15] L. Salasnich, A. Parola, and L. Reatto, Phys. Rev. A **66**, 043603 (2002); L. Salasnich, Phys. Rev. A **70**, 053617

- (2004).
- [16] P. Nozières and D. Pines, *The Theory of Quantum Liquids, Vol. II* (Addison-Wesley, Redwood City, 1990).
  - [17] P. A. Ruprecht, M. J. Holland, K. Burnett, and M. Edwards, Phys. Rev. A **51**, 4704 (1995).
  - [18] A. Gammal, T. Frederico, and L. Tomio, Phys. Rev. A **64**, 055602 (2001).
  - [19] V. I. Yukalov and E. P. Yukalova, Phys. Rev. A **72**, 063611 (2005).
  - [20] Using an appropriate initial guess, propagation of the GPE in imaginary time will converge to the ground state of the system, provided it exists.
  - [21] V. M. Perez-Garcia, H. Michinel, and H. Herrero, Phys. Rev. A **57**, 3837 (1998).
  - [22] When BSWs do not emerge from a collision we assign  $v_{\text{out}} = 0$ .
  - [23] Typically the peak density increases by a factor of 8 (2) for  $\Delta\phi = 0$  ( $\pi$ ).
  - [24] Population transfer and speed change are typically of the order of 1%.